Research Article

Na Su*

Preparation and performance of retention and drainage aid made of cationic spherical polyelectrolyte brushes

https://doi.org/10.1515/epoly-2022-0066
received April 30, 2022; accepted July 18, 2022

Abstract: Spherical polymer brushes were synthesized by grafting acrylamide from the surface of γ-methacryloxypropyl trimethoxy-silane-modified SiO_2 nanoparticles. Then, cationic spherical polyacrylamide (CSPAM) brushes were obtained by a manniched polyacrylamide (PAM). Fourier-transform infrared spectroscopy, transmission electron microscopy, thermogravimetric analysis, and gel permeation chromatography were introduced to analyze the structure, morphology, and molecular weight of CSPAM, respectively. The effects of pH and the dosage of CSPAM on the flocculation of fine pulp and precipitated calcium carbonate were studied. Furthermore, the optimal drainage performance could be achieved when the beating degree (°SR) decreased by about 14.42% with the dosage of CSPAM of 2 $mg \cdot g^{-1}$. The retention effect of CSPAM revealed that the highest first-pass retention was 71.1% when the dosage of CSPAM was 3.5 $mg \cdot g^{-1}$. In addition, the mechanism of retention and drainage of CSPAM was discussed.

Keywords: CSPAM, retention and drainage aid, flocculation, papermaking

1 Introduction

Driven by the rapid development of the papermaking industry, wet-end chemistry changes with each passing day. Among them, auxiliary materials, which are always of concern, have been widely used in papermaking for a long time and have played a pivotal role. Since the 1970s, acrylamide (AM) polymers (1,2), chitosan and its derivatives (3,4), cationic starch (5,6), etc. have been widely used in the paper industry, and dual retention systems (7,8) and microparticle retention systems (9,10) have also begun to emerge. In recent years, in order to relieve the integrated pressure of energy, resources, and the environment, the paper machine has become high-speed gradually, while the usage of herbage and wastepaper is increasing. It highlights the disadvantages of traditional additives. Consequently, the development of novel and efficient retention and drainage aids arouses general interest.

Spherical polyelectrolyte brushes (SPBs) with unique properties, such as high charge density, high symmetry or quasi-symmetric structure, and low molecular weight, provide great potential and limitless possibilities for their applications in biocompatibility (11), carrier system of nanoparticles (12), etc. In papermaking, the commonly used wet-end additives are cationic polymers, including poly(diallyldimethylammonium chloride) (13), 3-chloro-2-hydroxypropyltrimethyl ammonium chloride (14), poly [*N*,*N*,*N*-trimethyl-*N*-(2-methacryloxyethyl)ammonium chloride] (15), and cationic starch (16). If the polyelectrolyte chains affix to the sphere's surface, then novel cationic retention and drainage aids, namely cationic spherical polyelectrolyte brushes (CSPB), result. With their unique spherical structure, the shear resistance of spherical brushes is greater than that of linear polymers. Due to the introduction of more cationic groups on the molecular chain, the interaction between CSPB and slurry is enhanced, bringing about a better retention and drainage effect (17).

Spherical polyacrylamide brushes (SPAM), for example, quaternized SPAM will be more easily adsorbed on the fiber surface, resulting in the aggregation of fine fibers as well as the retention of negatively charged inorganic fillers. Consequently, quaternized SPAM is a potentially excellent additive in the papermaking industry. In this article, SPAM was first prepared by grafting PAM onto the surface of the modified SiO_2 using conventional free

* **Corresponding author: Na Su,** Department of Printing and Packaging Engineering, School of Shanghai Publishing and Printing College, Shanghai 200093, China; University of Shanghai for Science and Technology, Shanghai 200125, China, e-mail: suna@whu.edu.cn

radical polymerization. Then, the cationic modification of SPAM was achieved by Mannich reaction. Fourier-transform infrared spectroscopy (FTIR), transmission electron microscopy (TEM), thermogravimetric analysis (TGA), and gel permeation chromatography (GPC) were introduced to analyze the structure, morphology, molecular weight, and grafting density of the products. Furthermore, the retention and drainage performance and flocculation mechanism of cationic spherical polyacrylamide (CSPAM) were also discussed.

2 Experiment

2.1 Materials

2,2-Azobisisobutyronitrile (AIBN; Shanghai Chemical Co., Ltd), recrystallized from ethanol and dried under vacuum; AM (Guoyao Group of Chemical Reagents Ltd); ammonia ($NH_{3(aq)}$, 25–28 wt%); formaldehyde ($PA_{(aq)}$, 36–40 wt%; Guoyao Group of Chemical Reagents Ltd); dimethylamine ($DAM_{(aq)}$, 33 wt%; Guoyao Group of Chemical Reagents Ltd); hydrochloric acid (HCl, 34 wt%); ethanol; dimethyl sulfate; toluene; sodium hydroxide; sodium chloride; and distilled water were used. All chemicals and solvents used in this study were of analytical grade.

Precipitated calcium carbonate (PCC) with an average particle size of 5.68 μm, settling volume of 2.54 $mL \cdot g^{-1}$, and a specific surface area of 11.1 $m^2 \cdot g^{-1}$ was purchased from Yueyang Forest and Paper Co., Ltd (Hunan, China). Reed pulp provided by Dafeng Paper Group Co., Ltd was prepared to a 0.5 wt% pulp and its beating degree (BD) was set to 60°SR. The pulp suspension was separated into long fibers and fine fibers by a 200-mesh screen. All the slurries were stored at 4°C.

2.2 Synthesis of SPAM

The preparation method of modified silica microspheres was described elsewhere (18). The synthesis process of SPAM is shown in Figure 1. Briefly, 10 g of 4 wt% modified silica microspheres was first mixed with 100 mL of toluene and stirred in a three-necked bottle. The temperature was raised to 65°C under a nitrogen atmosphere. Following that, 300 mg of AM monomer and 18 mg of initiator (AIBN) were subsequently added to the mixture, followed by stirring for 6 h. The resulting products were separated and washed with distilled water and ethanol several times before being vacuum-dried at 60°C for 12 h.

Figure 1 also illustrates the procedure for cleaving long polymer chains from the surface of the modified SiO_2 nanoparticles. The hydrolysis reaction of SPAM was carried out by refluxing it in 2 M of $NaOH_{(aq)}$ at 85°C for 48 h. The reaction mixture involving SiO_2 cores and grafted polymer brushes was then carefully isolated by centrifuging. The PAM chains were acquired by extraction, neutralization, and concentration of the supernatant.

2.3 Cationization of SPAM

The cationization process of SPAM was achieved by Mannich reaction (19). First, when SPAM was allowed to react with formaldehyde in an alkaline solution, methylol derivatives were obtained. Tertiary amines were then

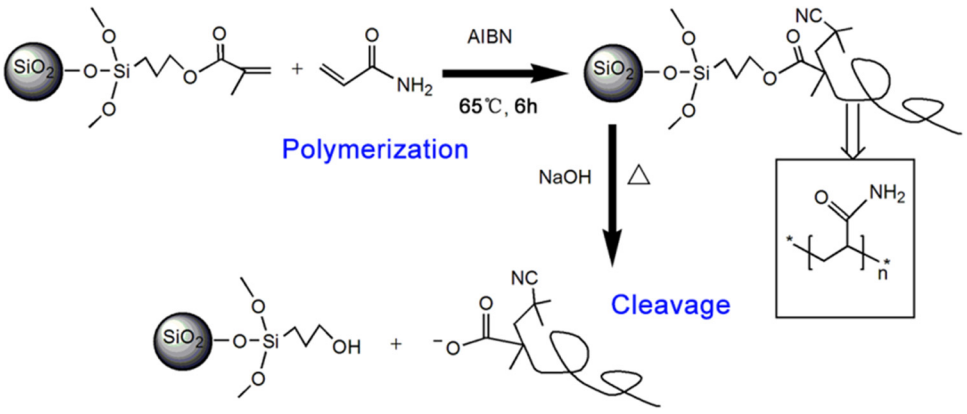

Figure 1: Synthesis process of SPB and hydrolysis of PAM chains.

generated by the reactions of methylol derivatives with dimethylamine. Finally, the resultant product reacted with dimethyl sulfate, thus obtaining cationized spherical PAM. The reaction process is schematically described in Figure 2.

About 1.0 g of SPAM was suspended in 10 mL of distilled water and ultrasonically dispersed. Subsequently, 130 mg of formaldehyde was added and adjusted the pH value of the suspension to 10 with sodium hydroxide solution. After the mixture was stirred at 50°C for 0.5 h, 3.5 mL of an aqueous solution containing 230 mg of dimethylamine was slowly added dropwise to the reaction mixture. The reaction was continued for 2.5 h. The temperature was then lowered to 30°C, followed by the dropwise addition of 180 mg of dimethyl sulfate dissolved in 6.5 mL of distilled water. The reaction was carried out for 1 h. Finally, the sample was centrifuged, and the resulting solid mixture was washed with an abundance of distilled water several times before being vacuum-dried at 65°C.

3 Characterization

3.1 FTIR and X-ray photoelectron spectroscopy (XPS)

FTIR was recorded using a Fourier-transform infrared spectrometer (Nicolet AVATAR 360 FT, USA) in a wavenumber range of 4,000–400 cm^{-1}. XPS measurements were carried out on an FEI "Quanta 200" instrument operating at a voltage of 30 kV with MnKα radiation.

3.2 Scanning electron microscopy (SEM) and TEM

SEM images were performed using a high-resolution Quanta 200 scanning electron microscope operated at 30 kV. TEM was recorded using a JEM-100CXII transmission electron microscope at an acceleration voltage of 100 kV.

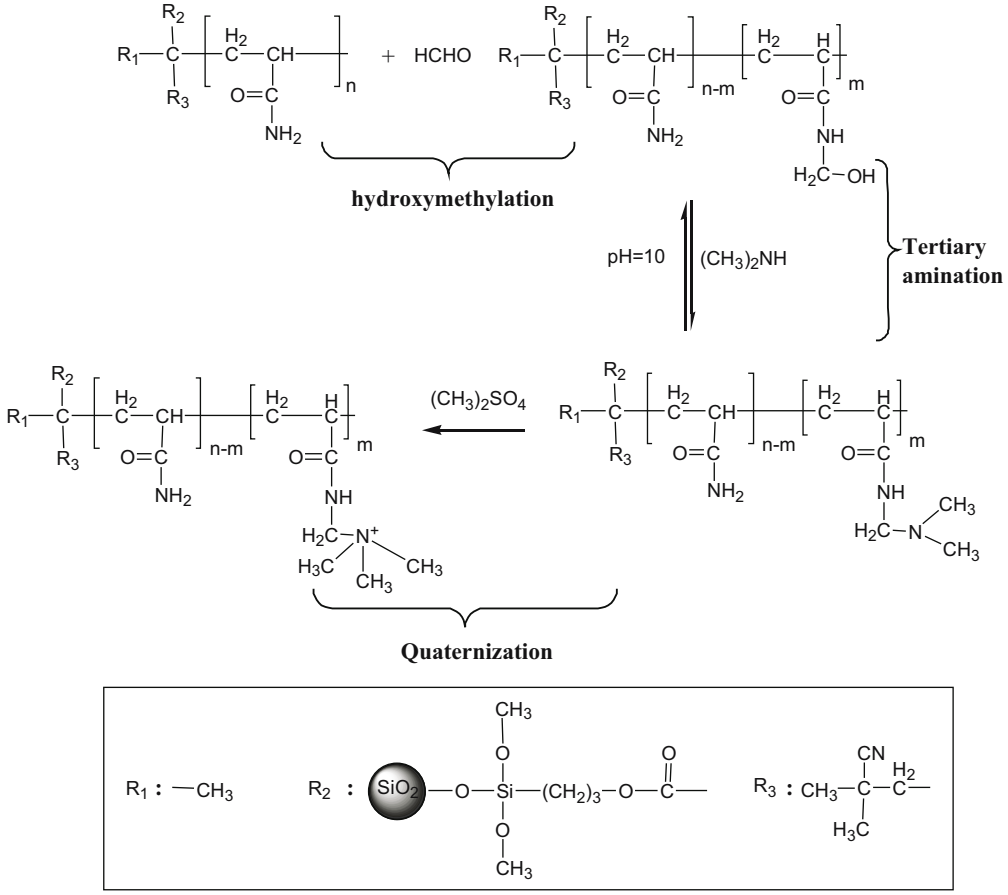

Figure 2: Schematic representation of cationization process of SPAM.

3.3 TGA

TGA was performed on a SETSYS-1750 (SETARAM Instrumentation, Caluire, Lyon, France) instrument at a heating rate of 10°C·min^{-1} under a nitrogen flow. The weight of all grafted PAM brushes (m) could be calculated by TGA. The initial mass of the sample was ca. 5 mg.

3.4 GPC

GPC was conducted on Spectra SERIES P100 to investigate the molecular weight distribution of PAM brushes. If the weight of all grafted PAM brushes (m) and the average molecular weight (M_w) are supplied, then the surface grafting density, σ, can be defined by the following equation (20):

$$\sigma = \frac{m}{4\pi r_c^2 \times M_w} \quad (1)$$

3.5 Dynamic light scattering (DLS) and charge density

The hydrodynamic radius R_h of SPB was analyzed by DLS using a particle sizer (Nicomp 380, USA), 25°C. A particle charge detector (Mütek PCD 03, Germany) was utilized to measure the charge density of samples.

A certain quantity of CSPAM was diluted to the required concentration with distilled water. After filtration, 10 mL of suspension was pipetted onto the measuring cell of particle change detector. All the samples were titrated with 0.001 M sodium polyethylene sulfate to the endpoint.

3.6 Flocculation of fine pulp and PCC suspension

Taking 30 mL of fine suspension, an amount of CSPAM was added, followed by adjusting the pH value of the reaction mixture with an aqueous solution of sodium hydroxide. The mixture was stirred for 30 s and was allowed to stand for 30 min. The transmittance of the supernatant at 550 nm was then measured photometrically by a spectrophotometer (Shimadzu UV-3600, Japan) subsequently.

In 30 mL of 0.01 mol·L^{-1} sodium chloride solution, 0.6 g of PCC was added. The suspension was continually stirred at room temperature for 2 min and ultrasonically defoamed for 5 min, followed by the addition of CSPAM after 24 h. After stirring for 3 s, the suspension was allowed to settle for 30 min. The value of the transmittance of the supernatant at 550 nm was investigated.

3.7 Retention and drainage

A certain amount of CSPAM suspension was added to 1,000 mL of reed pulp containing 2.0 g of dry pulp and stirred evenly. The BD was measured on a BD tester of Schopper-Riegler (ZQS12-100). Since the volume of water flowing through a pipe (V, mL) could be collected, the BD was calculated based on the following equation:

$$\mathrm{BD} = \frac{1{,}000 - V(\mathrm{mL})}{10} \quad (°\mathrm{SR}) \quad (2)$$

The first-pass retention (FPR) of pulp suspension and PCC was investigated by a Dynamic Drainage Jar (DDJ; MT2110-086CF, USA) with a 200-mesh screen. At a stirring speed of 600 rpm, 500 mL of pulp suspension was added to the DDJ. Subsequently, 0.56 mL of alkyl ketene dimer, 0.625 g of PCC, and the required amount of cationic spherical polyelectrolyte brush were added in sequence. The filtration time of 100 mL of first-pass white water was recorded, which was the water filtration efficiency. The filtrate (100 mL) was filtered, dried, and weighed. Then the amount of the remaining solid was calculated. The calculation method of FPR of pulp suspension is shown in the following (17):

$$\mathrm{FPR} = \frac{C_i - C_0}{C_i} \times 100\% \quad (3)$$

where C_i and C_0 are the concentrations of colloidal particles in slurry and filtrate, respectively.

4 Results and discussion

4.1 FTIR and XPS analyses

Figure 3 shows the FTIR spectra of SPAM (Figure 3a) and CSPAM (Figure 3b). As shown in Figure 3a, the appearance of a peak at 1,667.31 cm^{-1} can be attributed to the –C═O stretching vibration of the amide group (–$CONH_2$), confirming the presence of PAM (21). As can be seen from Figure 3b, the peaks at 1,469.85 and 953.63 cm^{-1} are assigned to the methylene group on –CH_2–$N^+(CH_3)_3$ and the methyl group on –$N^+(CH_3)_3$ stretching vibration,

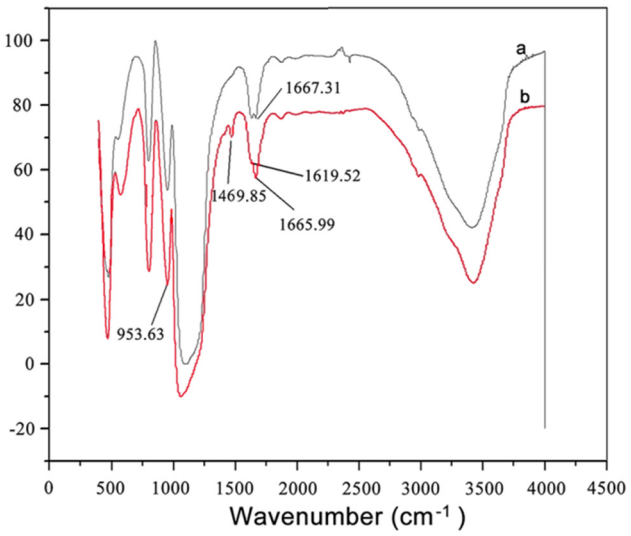

Figure 3: FTIR spectra of (a) SPAM and (b) CSPAM.

respectively (22,23), while the band located at 1,619.51 cm^{-1} belongs to $-NH_2$ in-plane bending vibration, demonstrating the successful cationization of PAM.

Figure 4 shows typical XPS wide-scan spectra for modified SiO_2 (Figure 4a) and CSPAM (Figure 4b). The nitrogen signals appear in the survey spectrum of CSPAM. The binding energy peaks at 399.8 eV (–CONH–) and 402.7 eV ($-N^+(CH_3)_3$) further support the surface modification and cationization reaction.

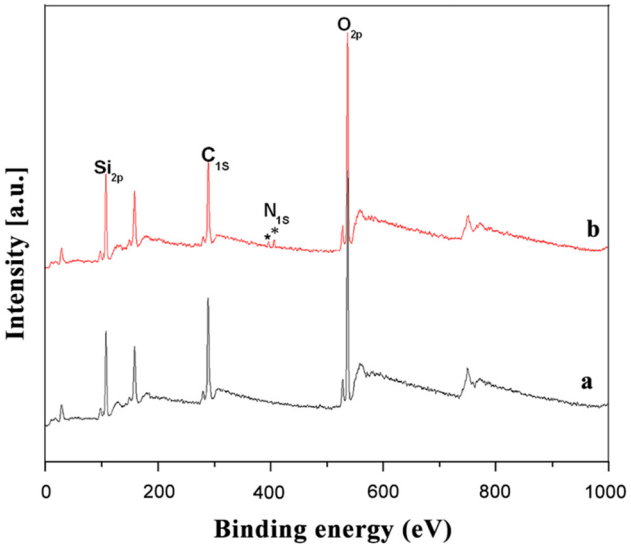

Figure 4: XPS spectra of wide region spectroscopy: (a) modified SiO_2 and (b) CSPAM.

4.2 SEM and TEM images

TEM and SEM images clearly demonstrate the morphologies of modified silica and SPAM. It can be seen from Figure 5 that the synthesized product has good dispersibility and has a stable and uniform spherical structure. The average diameter of SiO_2 cores is about 100 nm (Figure 5a), which is consistent with the results of the DLS determination (Figure 5e). In the TEM and SEM images of the synthesized SPAM (Figure 5b and d), fuzzy edges and hairs can be seen, proving the existence of PAM brushes. The results measured by DLS experiments showed that the thickness of the brush layer of the synthesized SPAM is 33 ± 2 nm (Figure 5f). It is further proved that AM chains have been successfully anchored on the surface of the modified silica particles.

4.3 TGA

In order to estimate the weight of grafted PAM brushes on the surface of modified SiO_2 cores, the TGA curves of modified SiO_2 and SPAM are described in Figure 6. It is shown that the weight loss below 200°C for the two curves means a loss of absorbed water. The weight loss of modified SiO_2 between 200°C and 750°C is about 9.4% (Figure 6a). The stage from 200°C to 750°C in Figure 6b mainly implies the loss of PAM brushes (10.7%). Therefore, the weight of all grafted PAM brushes could be investigated from Eq. 1.

4.4 Grafted polymer molecular weight and graft density

The molecular weight distribution of cleaved polymer chains from the surface of the modified SiO_2 nanoparticles is measured by GPC. The GPC curve of cleaved PAM chains is shown in Figure 7. Taking 0.1 M of $NaCl_{(aq)}$ as a buffer solution, polyethylene glycol (PEG) is used as the internal standard at room temperature. The results from the GPC measurement disclose that M_w and polydispersity (M_w/M_n) are 1.9×10^3 g·mol^{-1} and 1.6, respectively. The surface graft density calculated from Eq. 1 is 2.24×10^{-3} μmol·nm^{-2}. The charge density of CSPAM determined by colloid titration is 98.7 eq·L^{-1}.

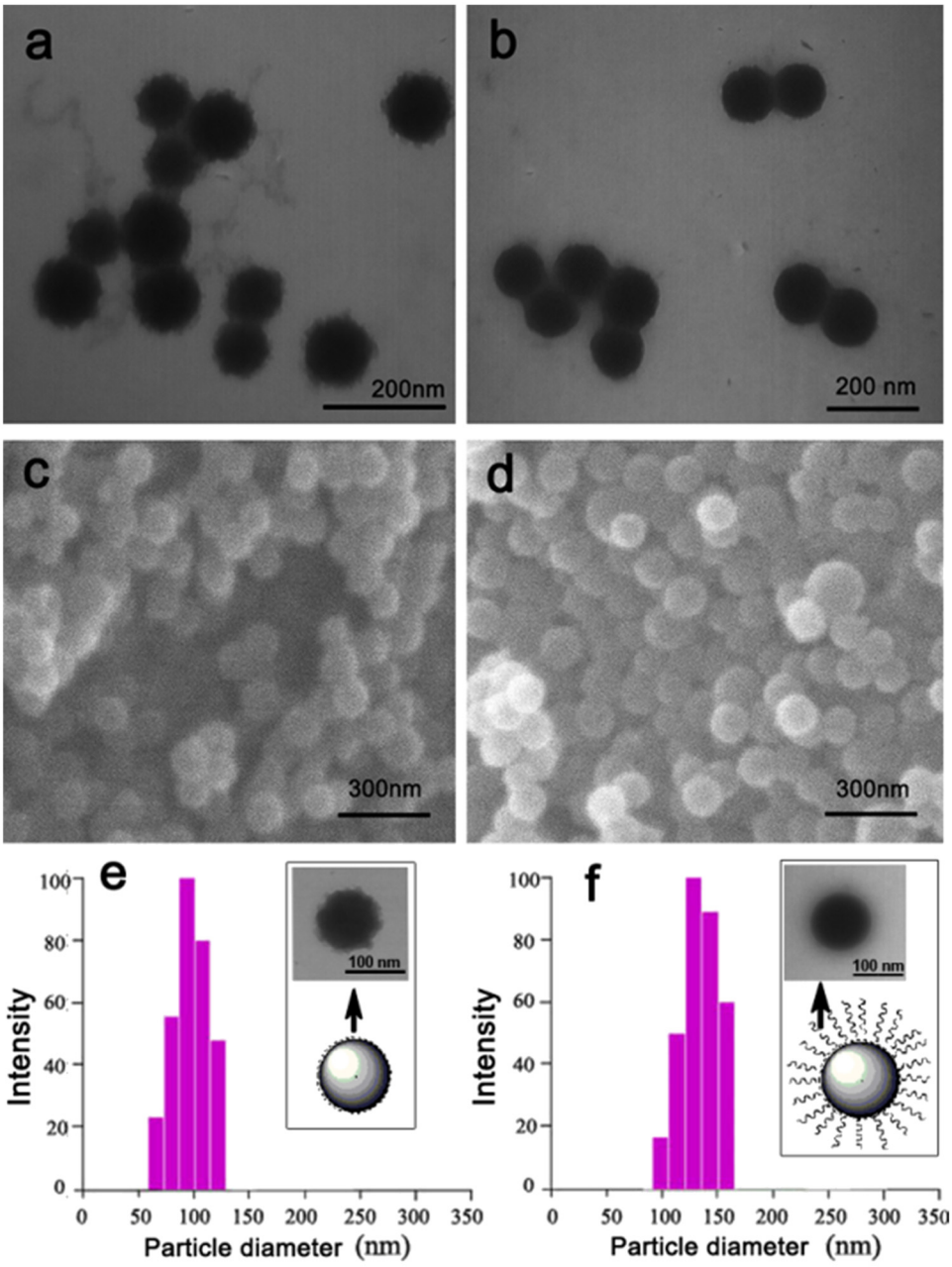

Figure 5: TEM images of (a) modified SiO_2 and (b) SPAM; SEM images of (c) modified SiO_2 and (d) SPAM; DLS curves of (e) modified SiO_2 and (f) SPAM.

4.5 Flocculation of fine pulp and PCC

The effects of pH value and the amount of CSPAM on the transmittance of the supernatant of fine pulp and PCC are presented in Figure 8. As shown in Figure 8a, a lower transmittance is available with a higher pH value of the system. This can be understood by the fact that a high pH value increases the negative potential on the surface of fine fibers. The increased repulsion between fibers enhances the stability of the system, causing a decreased transmittance (24). The largest transmittance value is obtained when the amount of additives is 10 $mg \cdot g^{-1}$ (63.2%, pH = 7). The reason for this may be that the positively charged CSPAM is close to the negatively charged fine pulp fibers by electrostatic attraction. With the increase in the amount of CSPAM, the local reversal of surface charge happens due to its high charge density (25). However, excessive amounts of additives will reduce the supernatant transmittance, which

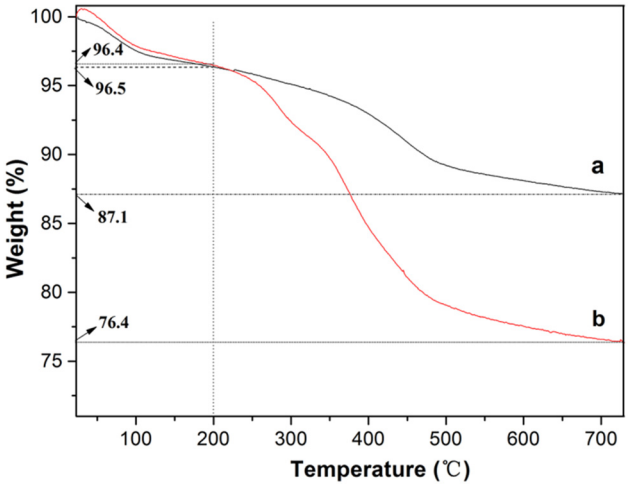

Figure 6: TGA of (a) modified SiO_2 and (b) SPAM.

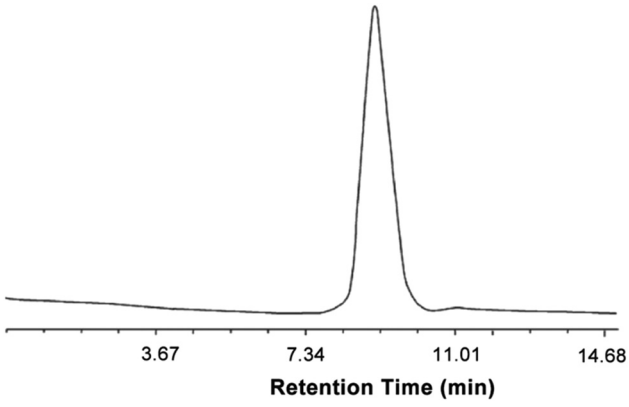

Figure 7: GPC curve of cleaved PAM chains.

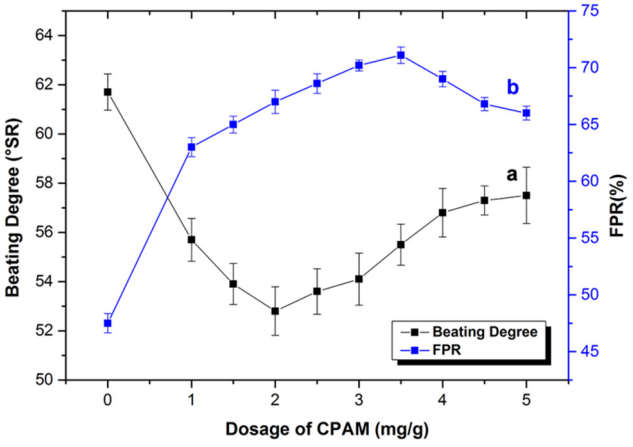

Figure 9: Effects of dosage of CSPAM on (a) BD and (b) FPR.

could be due to the occurrences of reversal potential and restabilization of the fine fibers.

Similarly, as shown in Figure 8b, the pH value of PCC suspension also influences flocculation. Under the same conditions, the transmittance of PCC suspension measured at pH = 9 is higher than those at pH values of 7 and 8. It may be the reason that the high pH value of the system reduces the solubility of PCC particles, resulting in poor stability of the system. Rapid precipitation of PCC particles occurs, thereby increasing the transmittance of the supernatant. In addition, the transmittance of the system increases with increasing CSPAM dosage and reaches the maximum improvement of 77.3% when the dosage of CSPAM is 2 $mg \cdot g^{-1}$ (pH = 9), which means that the optimal flocculation is achieved. The reason for this may be that positively charged CSPAM approaches the

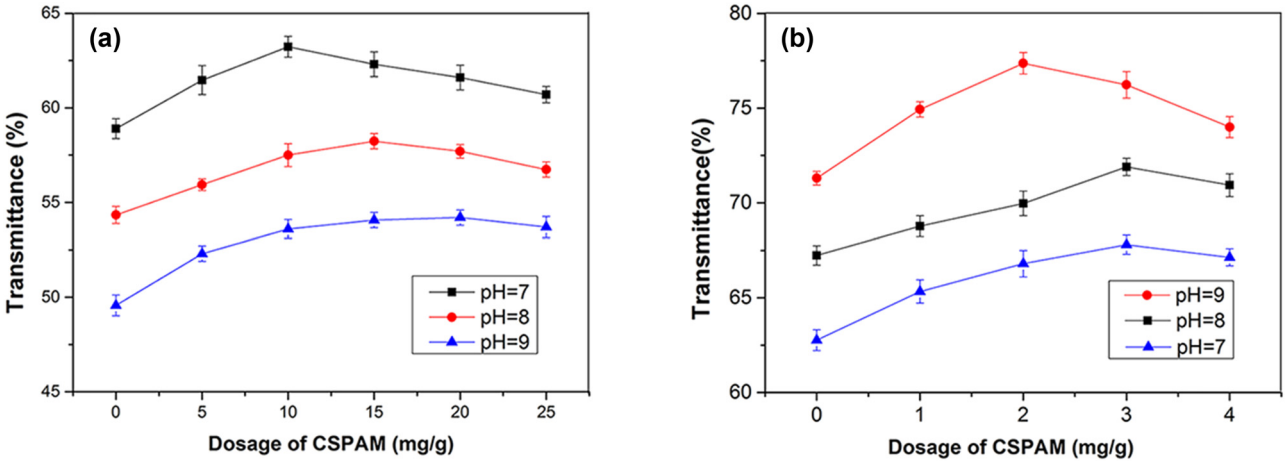

Figure 8: Effects of dosage of CSPAM on the transmittance of the supernatant of (a) fine pulp and (b) PPC (pH = 7, 8, 9).

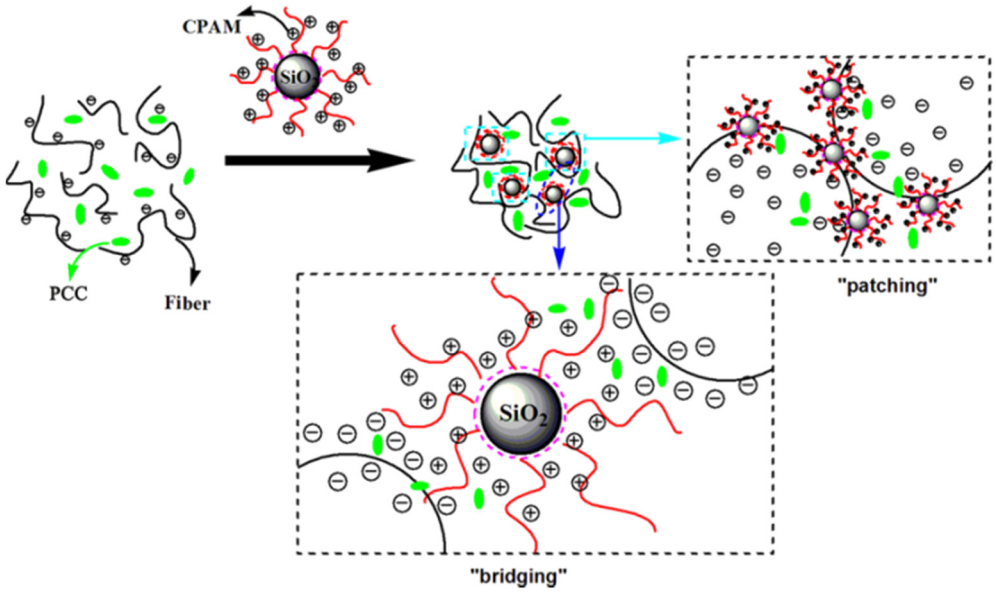

Figure 10: Flocculation mechanism of CSPAM.

negatively charged PCC particles through electrostatic attraction, and then the flocculation of PCC particles happens. However, excessive dosage of CSPAM will restabilize the PCC particles due to reversed surface potential, resulting in a decrease in transmittance.

4.6 Retention and drainage performance

Figure 9a illustrates the BD as a function of CSPAM at different dosages. It is shown that the magnitude of BD decreases with increasing CSPAM dosages. When the dosage of CSPAM is 2 $mg \cdot g^{-1}$, BD decreases by about 14.42% (52.8°SR), which means that optimal filtration performance is produced. This is because the reduced surface charge of the fibers after adding additives causes a decrease in the polarity and hydrophilicity of fibers, thus resulting in reduced adhesion and resistance. However, the redundant dosage of additives results in reversed charge and deteriorated flocculation, filtration performance decreases accordingly.

In Figure 9b, the FPR is improved from 47.5% to 71.1% when the dosage of CSPAM reaches 3.5 $mg \cdot g^{-1}$. In comparison with linear polymers, the drainage performance of branched polymers is significantly improved, which is consistent with the literature (26). FPR begins to decrease after adding a massive dosage of CSPAM. The reason for this is mainly that electrostatic interaction prevails with the addition of CSPAM leading to the aggregation of pulp cellulose. If more CSPAM is added, then the charge reversal phenomenon occurs, resulting in the deterioration of flocculation and a decrease in FPR (27).

4.7 Flocculation mechanism

Figure 10 describes the flocculation mechanism of CSPAM. According to the bridging theory, a bridging formation between CSPAM and multiple suspended particles on the surface of fibers is produced. Then the size of flocs increases significantly. Due to the adsorption of CSPAM onto the surface of fillers or fibers, the flocculation is generated by the CSPAM system. As a retention aid, CSPAM can be adsorbed on the surface of fibers in an extended structure (Figure 5b and f), forming a charge center. Therefore, the electrostatic attraction between CSPAM and fine fibers and fillers occurs. Moreover, compared with a flat layer surface, a more appropriate conformation may be adopted by flexible polymer brushes to fit the rugged surface of fibers and $CaCO_3$ particles. As a result, CSPAM plays the role of “bridging” as well as “patching.”

5 Conclusions

The CSPAM consisting of a modified SiO_2 core and a shell of CPAM has been prepared successfully. Different characterization and analytical methods clearly support polymerization and cationization reactions. Then the flocculation,

retention, and drainage performance of CSPAM on fine pulp and PCC are discussed. Results indicate that when the dosage of CSPAM is 10 $mg \cdot g^{-1}$ (pH = 7) and 2 $mg \cdot g^{-1}$ (pH = 9), the optimal flocculation effect is obtained for fine pulp and PCC, respectively. Moreover, optimal filtration performance and FPR are achieved at the condition of the dosage of CSPAM 2 and 3.5 $mg \cdot g^{-1}$, separately. Furthermore, the flocculation mechanism of CSPAM can be explained by the models of "patching" and "bridging."

Acknowledgement: The author acknowledges the technical support from the Key Lab of Intelligent and Green Flexographic Printing (KLIGFP-03).

Funding information: This work is sponsored by the Natural Science Foundation of Shanghai (21ZR1422100).

Author contributions: Na Su: writing – original draft, writing – review and editing, methodology, data curation, formal analysis, visualization, validation, and project administration.

Conflict of interest: The author states no conflict of interest.

Data availability statement: All data generated or analyzed during this study are included in this published article.

References

(1) Dong HY, Jung WJ, Woo C. Synthesis of cationic polyacrylamide/silica nanocomposites from inverse emulsion polymerization and their flocculation property for papermaking. Colloid Surface A. 2012;411(5):18–23. doi: 10.1016/j.colsurfa.2012.06.036.

(2) Nasser MS, Twaiq FA, Onaizi SA. Effect of polyelectrolytes on the degree of flocculation of papermaking suspensions. Sep Purif Technol. 2013;103:43–52. doi: 10.1016/j.seppur.2012.10.024.

(3) Guo KY, Gao BY, Tian XG, Zhang P, Shen X, Xu X. Synthesis of polyaluminium chloride/papermaking sludge-based organic polymer composites for removal of disperse yellow and reactive blue by flocculation. Chemosphere. 2019;231:337–48. doi: 10.1016/j.chemosphere.2019.05.138.

(4) Ruben M, Raluca N, Lsabel L, Mihail L, Elena B, Angeles B. Efficiency of chitosans for the treatment of papermaking process water by dissolved air flotation. Chem Eng J. 2013;231:304–13. doi: 10.1016/j.cej.2013.07.033.

(5) Chittapun S, Jangyubol K, Charoenrat T, Piyapittayanun C, Kasemwong K. Cationic cassava starch and its composite as flocculants for microalgal biomass separation. Int J Biol Macromol. 2020;161(15):917–26. doi: 10.1016/j.ijbiomac.2020.06.116.

(6) Niegelhell K, Chemelli A, Hobisch J, Griesser T, Reiter H, Hirn U, et al. Interaction of industrially relevant cationic starches with cellulose. Carbohyd Polym. 2018;179:290–6. doi: 10.1016/j.carbpol.2017.10.003.

(7) Santra S, Banerjee A, Das, B. Polycation charge and conformation of aqueous poly(acrylamide-*co*-diallyldimethylammonium chloride): Effect of salinity and temperature. J Mol Struct. 2022;1247:131292. doi: 10.1016/j.molstruc.2021.131292.

(8) Eva T, Gert D. On the inherent data fitting problems encountered in modeling retention behavior of analytes with dual retention mechanism. J Chromatogr A. 2015;1403(17):81–95. doi: 10.1016/j.chroma.2015.05.031.

(9) Cho BU, Garnier G, Theo GM, Perrier M. A deposition efficiency model for fiber–filler flocculation by microparticle retention system. J Ind Eng Chem. 2009;15(2):217–23. doi: 10.1016/j.jiec.2008.09.020.

(10) Fatemeh N, Hamidreza R, Hossein R, Hossein JT. Application of bio-based modified kaolin clay engineered as papermaking additive for improving the properties of filled recycled papers. Appl Clay Sci. 2019;182:105258. doi: 10.1016/j.clay.2019.105258.

(11) Czeslik C, Wittemann A. Adsorption mechanism, secondary structure and local distribution of proteins at polyelectrolyte brushes. Colloid Polym Sci. 2020;298:775–89. doi: 10.1007/s00396-019-04590-7.

(12) Ramasamy T, Tran TH, Cho HJ, Kim JH, Kim YI, Jeon JY, et al. Chitosan-based polyelectrolyte complexes as potential nanoparticulate carriers: physicochemical and biological characterization. Pharm Res. 2014;31:1302–14. doi: 10.1007/s11095-013-1251-9.

(13) Subramanian R, Zhu SR. Synthesis and flocculation performance of graft and random copolymer microgels of acrylamide and diallyldimethylammonium chloride. Colloid Polym Sci. 1999;277:939–46. doi: 10.1007/s003960050473.

(14) Aguado R, Lourenço AF, Ferreira PJ, Moral A, Tijero A. Cationic cellulosic derivatives as flocculants in papermaking. Cellulose. 2017;24:3015–27. doi: 10.1007/s10570-017-1313-y.

(15) Uematsu T, Matsui Y, Kakiuchi S, Isogai A. Cellulose wet wiper sheets prepared with cationic polymer and carboxymethyl cellulose using a papermaking technique. Cellulose. 2011;18:1129–38. doi: 10.1007/s10570-011-9536-9.

(16) Zhang XZ, Huang Y, Fu KQ, Yuan SJ, Huang C, Li HB. Preparation and performance of cationic flocculant for papermaking based on the graft polymerization of cationic chains from colloidal silica particles. Colloid Surface A. 2016;491:29–36. doi: 10.1016/j.colsurfa.2015.12.003.

(17) Mei Y, Abetz C, Birkert O, Schädler V, Leyrer RJ, Ballauff M. Interaction of spherical polyelectrolyte brushes with calcium carbonate and cellulose fibers: Mechanistic studies and their application in papermaking. J Appl Polym Sci. 2006;102(1):233–41. doi: 10.1002/app.23637.

(18) Su N, Li HB, Zheng HM, Yi SP, Liu XH. Synthesis and characterization of poly(sodium-p-styrenesulfonate)/modified SiO_2 spherical brushes. Eppress Polym Lett. 2012;6(8):680–6. doi: 10.3144/expresspolymlett.2012.72.

(19) Petasis NA, Akritopoulou I. The boronic acid mannich reaction: A new method for the synthesis of geometrically pure allylamines. Tetrahedron Lett. 1993;34(4):583–6. doi: 10.1016/S0040-4039(00)61625-8.

(20) Su N, Li HB, Huang Y, Zhang XZ. Synthesis of salt responsive spherical polymer brushes. J Nanomater. 2015;2015:1–7. doi: 10.1155/2015/956819.
(21) Feng J, Huang Y, Tu Z, Zhang H, Pan M, Tang H. Proton conduction of polyAMPS brushes on titanate nanotubes. Sci Reports. 2014;4:6225. doi: 10.1038/srep062251.
(22) Guo A, Geng Y, Zhao L, Li J, Liu D, Li P. Preparation of cationic polyacrylamide microsphere emulsion and its performance for permeability reduction. Pet Sci. 2014;11:408–16. doi: 10.1007/s12182-014-0355-0.
(23) Sun WM, Zhang GC, Pan L, Li HL, Shi A. Synthesis, characterization, and flocculation properties of branched cationic polyacrylamide. Int J Polym Sci. 2013;2013:1–10. doi: 10.1155/2013/397027.
(24) Liu Y, Zheng H, Wang Y, Zheng X, Wang M, Ren J, et al. Synthesis of a cationic polyacrylamide by a photocatalytic surface-initiated method and evaluation of its flocculation and dewatering performance: nano-TiO_2 as a photo initiator. RSC Adv. 2018;8:28329–40. doi: 10.1039/C8RA05622F.
(25) Huang Y, Zhang XZ, Fu KQ, Li HB, Huang C, Yuan SJ. Synthesis and application of cationic spherical polyelectrolyte brushes as retention and drainage aid in bleached eucalyptus kraft pulp. J Ind Eng Chem. 2015;31:309–16. doi: 10.1016/j.jiec.2015.07.003.
(26) Antunes E, Garcia FAP, Ferreira P, Blanco A, Negro C, Rasteiro MG. Use of new branched cationic polyacrylamides to improve retention and drainage in papermaking. Ind Eng Chem Res. 2008;47(23):9370–5. doi: 10.1021/ie801216t.
(27) Ono H, Deng Y. Flocculation and retention of precipitated calcium carbonate by cationic polymeric microparticle flocculants. J Colloid Interface Sci. 1997;188:183–92. doi: 10.1006/jcis.1997.4766.